

# Optimization of Flow Field Geometry in Proton Exchange Membrane Fuel Cell for Efficient Water Removal along Cathode to Improve Performance

Karthikeyan M

Fuel Cell Energy System Lab, Department of Automobile Engineering, PSG College of Technology, Coimbatore-641 004.

Magesh Kannan V

Fuel Cell Energy System Lab, Department of Automobile Engineering, PSG College of Technology, Coimbatore-641 004.

Vignesh M

Fuel Cell Energy System Lab, Department of Automobile Engineering, PSG College of Technology, Coimbatore-641 004.

Mathan C

Fuel Cell Energy System Lab, Department of Automobile Engineering, PSG College of Technology, Coimbatore-641 004.

Thanarajan K

Fuel Cell Energy System Lab, Department of Automobile Engineering, PSG College of Technology, Coimbatore-641 004.

Dineshkumar P

Fuel Cell Energy System Lab, Department of Automobile Engineering, PSG College of Technology, Coimbatore-641 004.

Karthikeyan P

Fuel Cell Energy System Lab, Department of Automobile Engineering, PSG College of Technology, Coimbatore-641 004.  
mkk.auto@psgtech.ac.in

## Abstract

This analysis is a three-pronged approach towards optimization of flow field geometry, reducing cathode flooding and improving the performance of Proton Exchange Membrane Fuel Cell (PEMFC). The performance of the fuel cell mainly depends on the flow field design. It is essential to optimize the flow geometry for each flow rate. This exertion numerically analyses three different variants of flow field geometry in PEMFC i.e., a 25 cm<sup>2</sup> PEM fuel cell with rib width by channel width of 2x2, a 25 cm<sup>2</sup> PEM fuel cell with slope of 1:50 & rib to channel ratio of 2:2, and finally a 36 cm<sup>2</sup> PEM fuel cell with slope of 1:20 & rib width by channel width of 1x1, using Computational Fluid Dynamics (CFD). This study uses hexahedral meshing for the geometry which will be more realistic when compared to those obtained in tetrahedral meshing. This primary step was carried out to enhance the performance of PEMFC within the ideal operating voltage range (0.4-0.6 V) such that the fuel cell can function in interference with the battery. The secondary step aims at reducing water formation in the interface between the rib and Gas Diffusion Layer (GDL). Stoichiometric ratio of 2.5 is used in experimentation and analysis, thus the tertiary step is to achieve a near stoichiometric reaction by optimization of flow geometry, thereby improving the fuel

cell performance. This trident numerical approach is done using FLUENT fuel cell module.

**Index Terms**— cathode flooding, numerically analyses, rib to channel ratio, slopes, hexahedral, stoichiometric .

## I. INTRODUCTION

FUEL CELLS are energy conversion devices which convert the chemical energy into electrical energy without any conventional conversion step. Fuel cells have advantages of relatively high conversion efficiency compared with conventional power sources, almost no pollution or emission during the operation, less moving parts, multiple choices of potential fuel sources and nearly instantaneous recharge capability compared to batteries [1]. Different fuels are used in fuel cells depending upon it's type. Fuel cells are generally classified according to the electrolyte used. Out of many types of fuel cells, Proton Exchange Membrane fuel cells also known as Polymer Electrolyte Membrane fuel cells, hereafter referred as PEM fuel cells, are the most commonly used fuel cells in automotive applications like cars, buses, submarines and airplanes. They are used as primary power source and also as auxiliary power source. The advantages

of PEM fuel cells are that they operate at low temperatures, start quickly, have more power to volume ratio and are flexible in orientation as compared to other types of fuel cells [2].

Typically a single PEM fuel cell consists of 9 layers: Anode current collector with grooved gas channels for flow of hydrogen, Anode Gas Diffusion Layer (GDL), Anode catalyst layer, Electrolyte membrane, Cathode catalyst layer, Cathode Gas Diffusion Layer and Cathode current collector with grooved gas channels for flow of oxygen / air.

Humidified fuel and oxidant are supplied in the gas channels, first these diffuse through the gas diffusion layers and then reaches the catalyst layer. At the interface of the membrane and the catalyst layer, the half-cell reaction takes place at both electrodes, at anode oxidation takes place, whereas reduction takes place at the cathode. The half reactions at anode and cathode are shown in equation (1) and equation (2) respectively. At the anode the hydrogen gas splits into protons and electrons, this specific membrane acting as an electrolyte allows only the protons to pass through while the electrons go around the external circuit. At the cathode, electrons and protons combine with oxygen to form water.

## II. PROJECT OBJECTIVE

The main objective of this work is to reduce the formation of water along the cathode and improving the performance of PEM Fuel cell. This phenomenon is known as flooding and hereafter addressed as cathode flooding.

The cathode flooding is one of the major problem in PEM fuel cell. Water or moisture plays a key role in the performance of PEM fuel cell. The membrane needs moisture for ionic conductivity and structural integrity. Decrease in water content leads to poor performance of fuel cell membrane whereas an increase in the water content can lead to flooding of the GDL and catalyst layers and also blocks the flow channel with water, thus reducing the re-activity rate. Thus maintaining a proper water balance is a very critical design parameter of PEM Fuel cell.

The cathode flooding can be reduced by using porous inserts [3,4] and/or modified design of flow channel [5,6]. In PEM fuel cell, there are different types of flow channel designs available. In which, Serpentine flow channel design has higher power output but also has higher cathode flooding rate and Parallel flow channel design has lower cathode flooding rate but low power output. So a fuel cell model of anode with serpentine flow channel design and cathode with parallel flow channel design is made to reduce the cathode flooding and improved power output. Further, a slope is added to cathode parallel flow channel design to facilitate water draining along cathode, which is likely to increase the PEM fuel cell performance.

## III. MODELING PROCEDURE

The following three fuel cell models are analyzed.

**Model 1** : A 25 cm<sup>2</sup> PEM fuel cell model, with both anode and cathode having serpentine flow channel and rib to channel ratio of 2:2, herein referred as Model 1, as shown in figure 1.

**Model 2** : A 25 cm<sup>2</sup> PEM fuel cell, with anode having

serpentine flow channel and cathode having parallel flow channel with slope of 1:50 and rib to channel ratio of 2:2, herein referred as Model 2, as shown in figure 2.

**Model 3** : A 36 cm<sup>2</sup> PEM fuel cell, with anode having serpentine flow channel and cathode having parallel flow channel with slope of 1:20 and rib to channel ratio of 1:1, herein referred as Model 3, as shown in figure 3.

### A. Design Phase

Design of above mentioned Fuel cell models are done using SOLIDWORKS 2012.

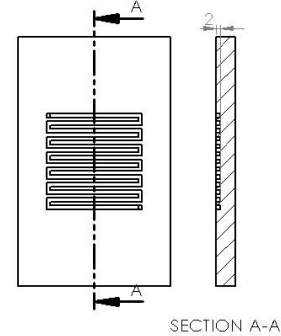


Figure 1. Serpentine flow channel design of graphite plate of Model 1 Fuel cell.

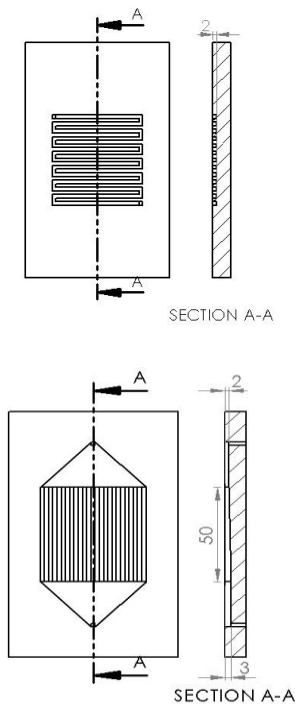


Figure 2. Anode (top) and Cathode (bottom) graphite plate of Model 2 Fuel cell.

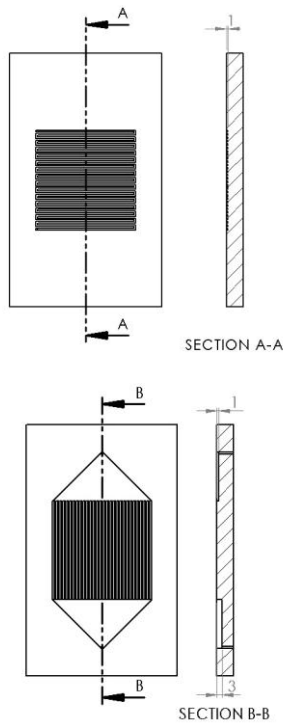


Figure 3. Anode (top) and Cathode (bottom) graphite plate of Model 3 Fuel cell.

The dimensions of the Membrane Electrode Assembly (MEA) are shown in Table I.

TABLE I MEMBRANE ELECTRODE ASSEMBLY DIMENSIONS

Components	Thickness
Catalyst Layer (Anode)	25 $\mu\text{m}$
Catalyst Layer (cathode)	50 $\mu\text{m}$
Gas Diffusion Layers	360 $\mu\text{m}$
Membrane	50.8 $\mu\text{m}$

### B. Meshing and Simulation Phase

Meshing of above designed fuel cell models are done using ICEM CFD.

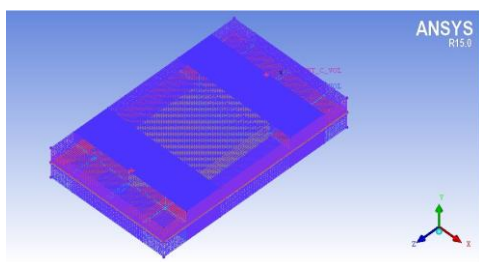


Figure 4. Meshing diagram of Fuel cell.

Tetrahedral cells are preferred for complex geometry because of ease of fitting in the volume but for relatively simple geometries of fuel cell, hexahedral elements are preferred because of their ability to generate a uniform and conformal mesh with lesser number of elements therefore in this study hexahedral elements were used. The details of the mesh are shown in Figure 4 and Figure 5.

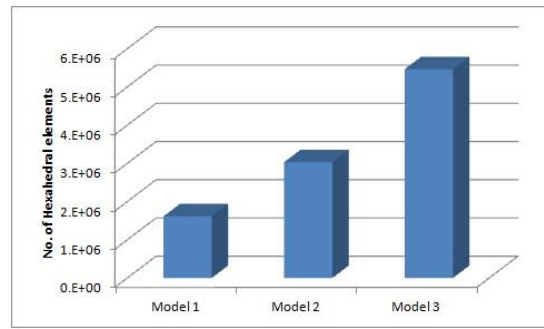


Figure 5. Meshing details of all three Fuel cell Models.

TABLE II MATERIAL PROPERTIES

Components	Property	Units	Current Study
<b>Bipolar plates</b>	Electrical conductivity	S/m	7500
	Thermal conductivity	W/m K	31.5
<b>Catalyst layers</b>	Active surface area per unit volume	$\text{m}^{-1}$	$2 \times 10^5$
	Electrical conductivity	S/m	1800
	Permeability	$\text{m}^2$	$1.45 \times 10^{-11}$
	Thermal conductivity	W/m K	12
	Porosity		0.112
<b>Gas diffusion layers</b>	Electrical conductivity,	S/m	1800
	Permeability	$\text{m}^2$	$1.45 \times 10^{-11}$
	Thermal conductivity	W/m K	12
	Porosity		0.4
	Density	$\text{kg}/\text{m}^3$	2719
<b>Electrolyte</b>	Equivalent weight	$\text{kg}/\text{kmol}$	1100
	Thermal conductivity	W/m K	0.36
	Electronic conductivity	S/m	$1 \times 10^{-16}$
	Density	$\text{kg}/\text{m}^3$	1980

Once the mesh were created and zones and surfaces are identified in ANSYS ICEM CFD, it was imported in the ANSYS FLUENT software. Material properties boundary conditions, initial conditions, operational conditions and modeling parameters were defined. The software computes the results of coupled non-linear equations [7].

Table II gives the material properties used for the fuel cell model and Table III gives the boundary conditions

applied for the fuel cell models respectively. The boundary conditions were selected and flow rates and mass fractions were calculated so as to match the experimental conditions.

TABLE III BOUNDARY CONDITIONS

Description	Units	Current Study	
Fuel cell Temperature	°C	60	
Anode humidification temperature	°C	60	
Cathode humidification temperature	°C	60	
Anode pressure	bar	4	
Cathode pressure	bar	4	
Anode flow rate	kg/s	$2 \times 10^{-6}$	
Cathode flow rate	kg/s	$6.08 \times 10^{-6}$	
Inlet mass fraction Anode	H <sub>2</sub>	%	34
	H <sub>2</sub> O	%	3
Inlet mass fraction Cathode	O <sub>2</sub>	%	89.09
	H <sub>2</sub> O	%	0.5
	N <sub>2</sub>	%	10.41

This study was carried out using fuel cell module [10] which leads to the assumptions of steady state, non-isothermal, multiphase flow in the GDL using mixture model and isotropic properties of the GDL and considers the following.

*Joule heating:* It takes the heat generated by charge transport in energy source term.

*Electrochemistry Sources:* It accounts for the electrochemistry effects in the model.

*Reaction heating:* It takes the heat generated by chemical reaction in energy source term.

*Butler-Volmer Rate:* It takes account of transfer currents inside the catalyst layers. Transfer currents are approximated by Tafel approximation when this option is not used.

*Multiphase:* It computes the approximate liquid water transport inside the Gas Diffusion Layer.

The solution controls are done by F-Cycle with BCGSTAB (bi-conjugate gradient stabilized method) was selected for the solution of the three species equations, electrical and potential equations and saturation equations.

The termination criteria were lowered from default 0.01 to 0.001 for species and saturation equations whereas the termination criteria for two potential equations are reduced further to 0.0001, as recommended by the ANSYS Inc. fuel cell module.

Another important parameter in numerical simulation is under-relaxation factor. In pressure-based solver, under-relaxation factor soothes the convergence behaviour of outer nonlinear iterations with the help of an additional multiple of the computed change in the quantity [8].

Lower values of under-relaxation factor results in slow convergence whereas high values of under relaxation factors can

result in divergence or an oscillating value of the solution. The most favorable value of under-relation factor depends upon how it's is required to be sought for each case differently [11]. In this study the under relation factor were fixed according to the recommendations of ANSYS FLUENT for fuel cell simulations initially and then tailored according to diverging or converging results in first few simulation runs[12]. The under relaxation factors were set finally as in Table IV.

An important indicator or solution convergence is the residual between two consecutive calculations. A declining graph of residual means, that the solution is progressing towards convergence whereas the increasing values of residuals indicate divergence. In this study, the solution was taken as converged when the mass continuity residual was in the order of  $10^{-3}$  and the difference between anode and cathode currents was less than  $0.0001 \text{ A/cm}^2$ .

#### IV. RESULTS AND DISCUSSION

Design and Simulation of all three Fuel cell Models are completed and their results are discussed below.

##### A. Validation of Simulation Results of Model 1 with the Experimental data

Validation of simulation results with the experimental data is required when pursuing a Numerical simulation.

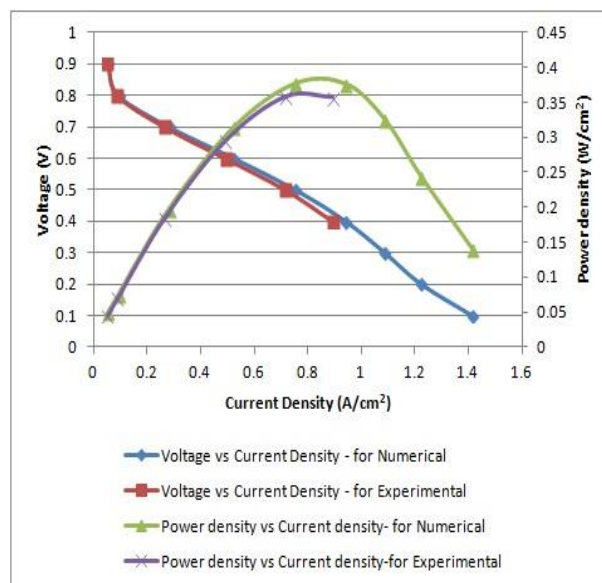


Figure 6. Comparison of Polarization and Performance Curve of Experimental data and Numerical results of Model 1.

It is clear from Figure 6, the polarization curve (voltage vs current density) and performance curve (power density vs current density) for numerical simulation of Model 1 matches with experimental results [9]. The average error percentage between them is around 5%.

**B. Comparison of Numerical results of Model 1 and Model 2**

Both the Numerical Results of Model 1 and Model 2 are compared below.

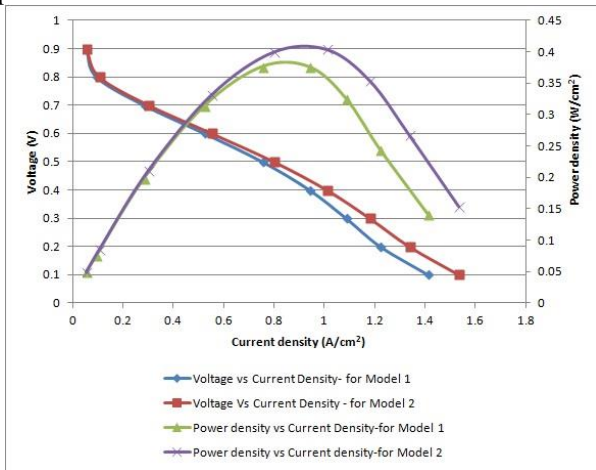


Figure 7. Comparison of Polarization and Performance Curve of Model 1 and Model 2.

From Figure 7, the polarization curve and performance curve of model 2, shows better results than that of model 1. So from that, we can say, increase in the slope of cathode channel, increases the performance of the fuel cell.

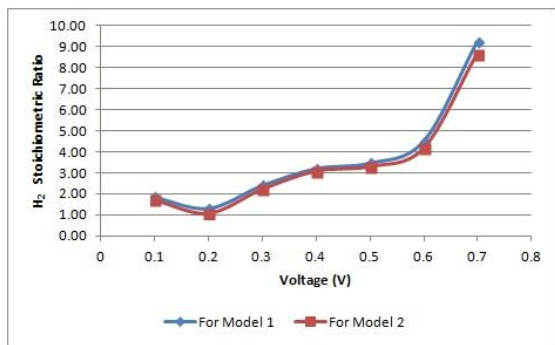


Figure 8. Comparison of H<sub>2</sub> stoichiometric ratio of Model 1 and Model 2 for different voltage.

Figure 8 shows the stoichiometric curve of model 1 and model 2 for different voltage. The fuel (H<sub>2</sub> gas) wastage of model 2 is lesser when compared to that of model 1. So from that we can say, increase in the slope of cathode channel, decreases fuel wastage.

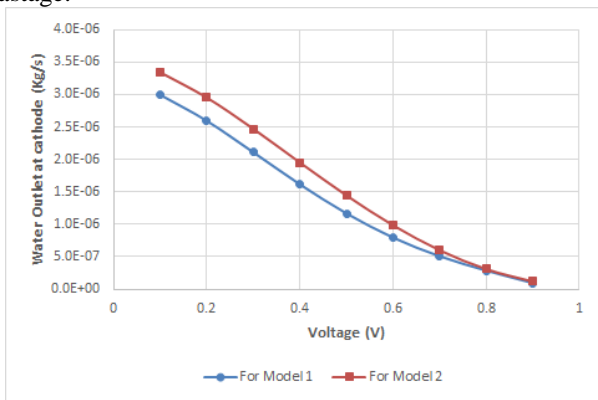


Figure 9. Comparison of Cathode channel water outlet of Model 1 and Model 2 for different voltage.

Figure 9 shows the water removal rate at cathode of model 1 and model 2 for different voltage. The water removal at cathode of model 2 is more when compared to that of model 1. So from that we can say, increase in the slope of cathode channel, will increase cathode water removal.

**C. Comparison of Numerical results of Model 2 and Model 3**

Both the Numerical Results of Model 2 and Model 3 are compared below.

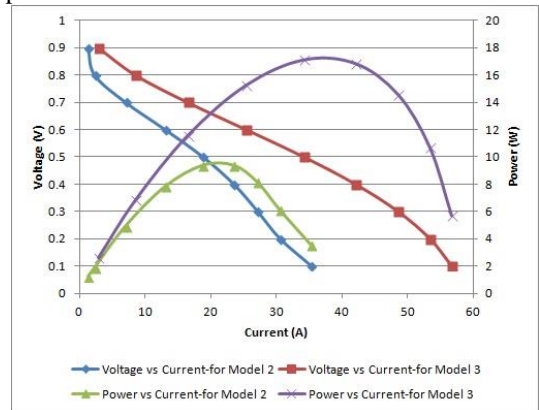


Figure 10. Comparison of Polarization and Performance Curve of Model 2 and Model 3.

Figure 10 shows the polarization curve and performance curve of model 2 and model 3. The polarization and performance curve of model 3 shows better results than that of model 2. So from that we can say, increase in the slope of cathode channel, decrease in rib thickness, increase in cell active area will increase the performance of the fuel cell.

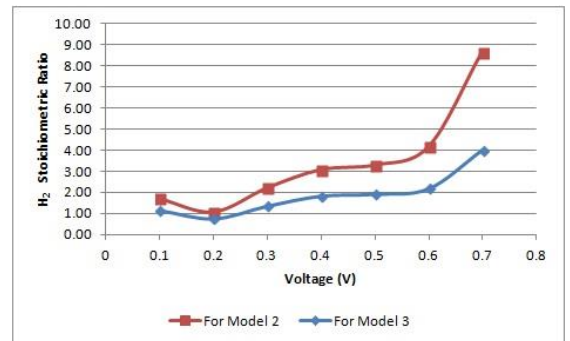


Figure 11. Comparison of H<sub>2</sub> stoichiometric ratio of Model 2 and Model 3 for different voltage.

Figure 11 shows the stoichiometric curve of model 2 and model 3 for different voltage. The fuel (H<sub>2</sub> gas) wastage of model 3 is lesser when compared to that of model 2. So from that we can say, increase in the slope of cathode channel, decrease in rib thickness, increase in cell active area will decrease fuel wastage.

Figure 12. Comparison of Cathode channel water outlet of Model 2 and Model 3 for different voltage.

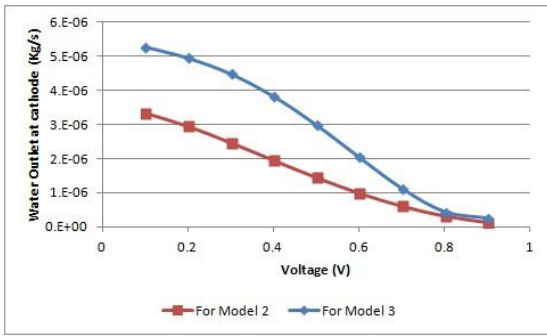


Figure 12 shows the water removal rate at cathode of model 2 and model 3 for different voltage. The water removal at cathode of model 3 is more when compared to that of model 2. So from that we can say, increase in the slope of cathode channel, decrease in the rib thickness, increase in cell active area, will increase cathode water removal.

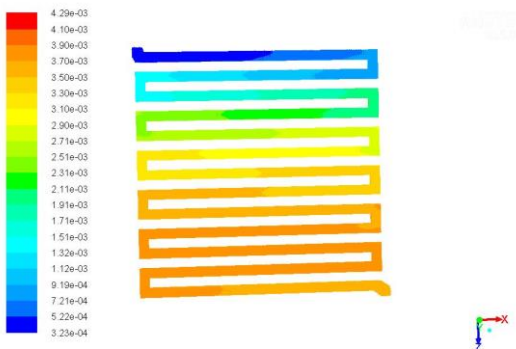


Figure 13(A).Molar concentration of H<sub>2</sub>O in cathode channel in model 1.

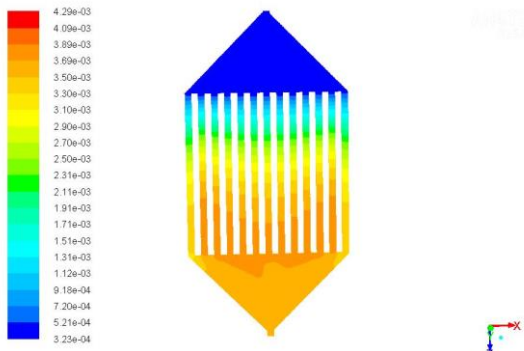


Figure 13(B).Molar concentration of H<sub>2</sub>O in cathode channel in model 2.

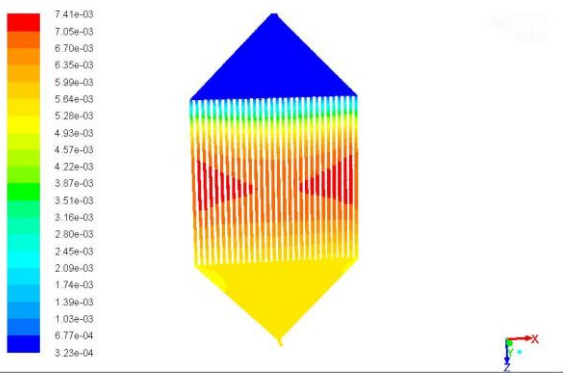


Figure 13(C).Molar concentration of H<sub>2</sub>O in cathode channel in

model 3.

Figure 13 (A), 13(B) and 13(C) are the graphic plot of molar concentration of H<sub>2</sub>O in cathode channel for models 1, 2 and 3.

From which we can say that, among the models considered cathode flooding rate is lesser for model 2 when compared to model 1, and least for model 3.

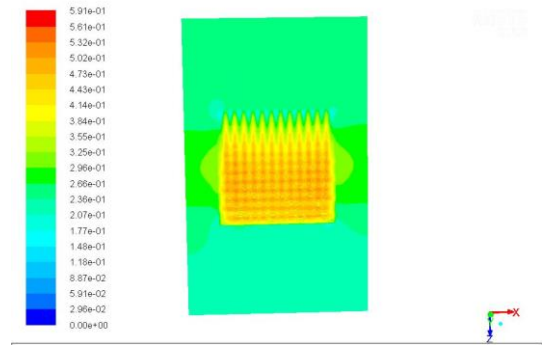


Figure 14(A).Membrane liquid water activity for model 1.

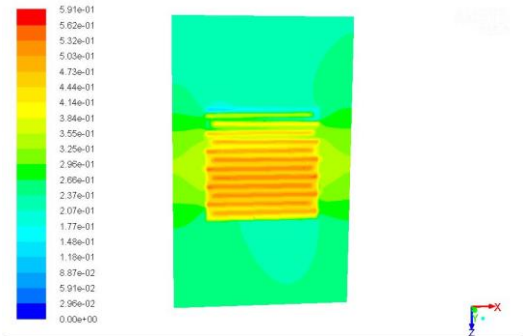


Figure 14(B).Membrane liquid water activity for model 2.

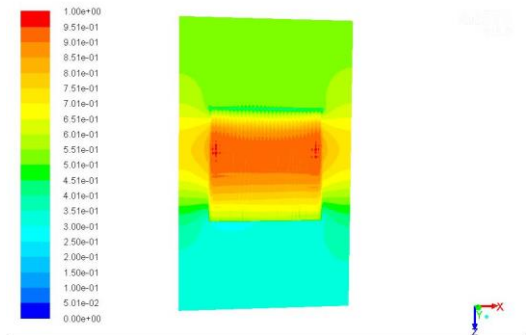


Figure 14(C).Membrane liquid water activity for model 3.

Figure 14(A), 14(B) and 14(C) shows liquid water activity in membrane for model 1, 2 & 3. Liquid water activity in membrane for model 2 is more when compared to that of model 1. Also liquid water activity in membrane for model 3 is more when compared to that of model 2 and model 3.

## V. CONCLUSION

From the results obtained, it's clear that the parallel flow channel with slope shows improved performance of PEMFC when compared to other flow channels and it also

effectively reduces the water formation along the cathode.

On further experimentation and detailed analysis of the results it's clear that by increasing the cathode parallel flow channel's slope and increase in active area of the cell or decreasing the rib thickness also improves the performance of the fuel cell and water formed along the cathode is also drained efficiently.

## REFERENCES

- [1] M.M. Mench, Fuel cell Engines, John Wiley & Sons Inc., 2008, 2, 3, 286.
- [2] J. Larminie, Fuel Cell Systems Explained, 2nd Ed, John Wiley & Sons Inc., 2003, pp67. Sivertsen 13.R., Djilali N., CFD-based modelling of proton exchange membrane fuel cells, Journal of Power Sources, 4 1, 2005, 65-75.G
- [3] M Karthikeyan, P Karthikeyan, M Muthukumar, V Magesh Kannan, K Thanarajan, T Maiyalagan, Chae-Won Hong, Vasanth Rajendiran Jothi, Adoption of novel porous inserts in the flow channel of pem fuel cell for the mitigation of cathodic flooding, International Journal of Hydrogen Energy, 2020, 45 (13), 7863-7872.
- [4] Muthukumar Marappan, Rengarajan Narayanan, Karthikeyan Manoharan, Magesh Kannan Vijayakrishnan, Karthikeyan Palaniswamy, Smagul Karazhanov, Senthilarasu Sundaram, Scaling up Studies on PEMFC Using a Modified Serpentine Flow Field Incorporating Porous Sponge Inserts to Observe Water Molecules, 2021, Molecules 26 (2), 286.
- [5] Magesh Kannan Vijayakrishnan, Karthikeyan Palaniswamy, Jegathishkumar Ramasamy, Thanarajan Kumaresan, Karthikeyan Manoharan, Thundil Karuppa Raj Rajagopal, T Maiyalagan, Vasanth Rajendiran Jothi, Sung-Chul Yi, Numerical and experimental investigation on 25 cm<sup>2</sup> and 100 cm<sup>2</sup> PEMFC with novel sinuous flow field for effective water removal and enhanced performance, International Journal of Hydrogen Energy, 2020, 45 (13), 7848-7862.
- [6] Muthukumar Marappan, Magesh Kannan Vijayakrishnan, Karthikeyan Palaniswamy, Karthikeyan Manoharan, Thanarajan Kumaresan, Jyothis Arumughan, Experimental investigation on serpentine, parallel and novel zig-zag flow fields for effective water removal and enhanced performance on 25 cm<sup>2</sup> PEMFC, 2021, Journal of Ceramic Processing Research 22 (2), 131-142
- [7] ANSYS FLUENT 12.0, -fuel Cells Module Manual, 2009, ANSYS Inc.
- [8] ANSYS FLUENT 1 2.0, Theory guide, 2009, ANSYS Inc.
- [9] P.Karthikeyan, P.Velmurugan, Abby Joseph George, R.Ram Kumar, R.J. Vasanth, Experimental Investigation on scaling and stacking up of proton exchange membrane fuel cell, International Journal of Hydrogen Energy 39 (2014) 11136-11195.
- [10] Yun Wong, Ken S.Chen, Jeffrey Mshler, Sung Chan Cho, Xavier Cordobes Adroher, A review of polymer electrolyte membrane fuel cells: Technology, applications, and needs on fundamental research, Applied Energy 88 (2011) 981-1007.
- [11] Rui B. Ferreira, D.S. Falcao, V.B. Oliveira, A.M.F.R. Pinto Numerical simulations of two-phase flow in proton exchange membrane fuel cells using the volume of fluid method - A review, Journal of Power Sources 277 (2015) 329-342.
- [12] Mihir M. Shah, Satish G. Kandlikar Water emergence from the land region and water sidewall interactions in Proton Exchange Membrane Fuel Cell gas channel with microgrooves, Journal of Power Sources 297 (2015) 127-139.